

## Vertical propagation of lakewide internal waves

Stephen M. Henderson<sup>1</sup> and Bridget R. Deemer<sup>1</sup>

Received 7 December 2011; revised 18 February 2012; accepted 22 February 2012; published 23 March 2012.

[1] Internal waves with diurnal period dominated velocities measured by an Acoustic Doppler Profiler (ADP) in a small lake (main basin 3000 m by 400 m by 18 m). ADP profiles and an along-lake temperature section indicate that the observed waves, like seiches, had horizontal wavelengths exceeding the metalimnion length. However, unlike non-dissipative seiches, the observed waves propagated vertically, carrying energy to the lakebed where waves were absorbed, rather than being strongly reflected. This absorption is predicted by a standard parameterization of boundary layer dissipation. The absence of upward-propagating energy precludes seiche resonance, limits focusing of waves toward attractors, and suggests that hypolimnion dissipation was limited by the supply of downward-propagating energy. Vertical wavelengths were less than the lake depth. Simplified calculations suggest that vertically-propagating waves, as opposed to vertically standing seiches, are most likely where vertical wavelengths are short, near-bed stratification is strong, and lakes are short and deep. **Citation:** Henderson, S. M., and B. R. Deemer (2012), Vertical propagation of lakewide internal waves, *Geophys. Res. Lett.*, *39*, L06405, doi:10.1029/2011GL050534.

### 1. Introduction

[2] Internal waves called seiches, often generated by fluctuating winds, dominate interior and near-bed flows in many lakes [Mortimer, 1952]. Seiche dissipation generates turbulence, which is responsible for mixing heat [Lorrai *et al.*, 2011], sediments [Pierson and Weyhenmeyer, 1994], chemicals [MacIntyre and Jellison, 2001], organisms [Serra *et al.*, 2007], and pollutants [Sorensen *et al.*, 2004].

[3] Seiches are often described using idealized non-dissipative theories for standing waves in rectangular basins with horizontal beds and vertical sidewalls. Often, seiche energy is dominated by the lowest horizontal mode, which has a horizontal wavelength exceeding the lake length. A series of possible vertical seiche modes have been predicted and observed [LaZerte, 1980; Münnich *et al.*, 1992; Pannard *et al.*, 2011]. Each vertical mode is a standing wave formed as internal waves generated by winds carry energy to the lakebed, reflect, and then carry energy back to the surface. If winds oscillate with the natural seiche period, non-dissipative theories predict resonant accumulation of energy through repeated cycles of surface forcing and vertical propagation [Mortimer, 1952; Vidal *et al.*, 2008].

[4] Sloping lakebeds complicate the simple theory outlined above [Thorpe, 1998]. Internal waves reflecting from the bed maintain a constant angle from vertical (Figures 1a–1d).

Consequently, angles of incidence and reflection are unequal, causing focusing or defocusing. For sufficiently low (“subcritical”) bed slopes, internal waves carrying energy down toward a lakebed are reflected upward (Figures 1a and 1b). Steeper (“supercritical”) slopes reflect waves downward (Figures 1c and 1d). Focusing can be intense when the bed slope is nearly critical [Eriksen, 1982; Gómez-Giraldo *et al.*, 2006]. Resulting “hotspots” of turbulent dissipation might mix heat, chemicals and organisms, and have been implicated in the shaping of continental shelves [Cacchione *et al.*, 2002]. Even if slopes are far from critical (but non-zero), non-dissipative theories predict that intense focusing can develop during repeated cycles of vertical propagation and reflection, with a small amount of focusing occurring during each cycle. In this case, waves propagate ever closer to trajectories called ‘Internal Wave Attractors’ (IWAs) [Maas and Lam, 1995]. To date, IWAs have been identified in the laboratory [Maas *et al.*, 1997; Hazewinkel *et al.*, 2010] but not in the field.

[5] The above discussion of focusing and resonance neglects dissipation, which is often concentrated in boundary layers near lakebeds [Wüest and Lorke, 2003]. Given sufficient dissipation, most wave energy carried to the bed could be absorbed rather than reflected. The resulting downward propagation of internal wave energy would be associated with upward propagation of wave phase [Phillips, 1977], in contrast with the vertically standing modes previously reported (weak vertical propagation has been simulated using coupled modes [Brink and Allen, 1978] for rectangular basins [Shimizu and Imberger, 2009]). Focusing on IWAs and seiche resonance both accumulate over multiple cycles of vertical propagation, and both might therefore be suppressed by boundary layer absorption.

[6] We present observations of vertically propagating, near-diurnal period internal waves in a narrow lake. After outlining the field site and instrumentation (section 2), observations of upward phase propagation (implying downward energy propagation) are presented (section 3). A simple analytic model predicted the observed vertical propagation speed. An along-lake temperature section was consistent with vertical wavelengths less than the lake depth, and horizontal wavelengths exceeding the lake length (section 4). Across-lake sections (section 5) suggest that Coriolis accelerations were approximately cancelled by across-lake baroclinic pressure gradients. Results are summarized and implications for hypolimnion mixing are discussed (section 6). A simple parameterization of boundary layer dissipation is shown to predict wave absorption at the lakebed.

### 2. Field Site and Instrumentation

[7] Measurements were collected in Lacamas Lake, Washington (Figure 1e) between 31 August and 23

<sup>1</sup>School of the Environment, Washington State University Vancouver, Vancouver, Washington, USA.

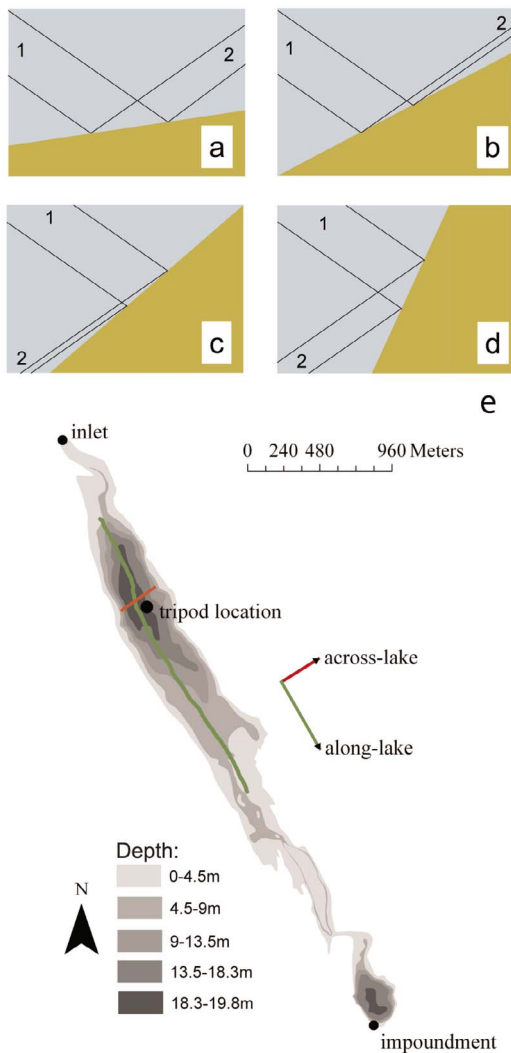


**Figure 1.** (a–d) Vertical sections through idealized bathymetry and (e) map of observed bathymetry showing CTD transects (red and green lines). In Figures 1a–1d, wave rays (black lines) reflect from a lakebed to maintain a constant angle from vertical. Slope is subcritical in Figures 1a and 1b and supercritical in Figures 1c and 1d. Propagation from 1 to 2 focuses energy (2 to 1 defocuses), particularly for near-critical slopes (Figures 1b and 1c).

September 2011. During this time, the depth of Lacamas Lake declined from about 18 m to 16.5 m, owing to a controlled dam spill. Water was spilled from the lake surface, reducing the thickness of a near-surface layer of warm water, but spill rates were too slow to generate measurable velocities in the deep lake or to significantly tilt the thermocline.

[8] Velocity was measured using an upward-looking 1 MHz Nortek Aquadopp Acoustic Doppler Profiler (ADP) mounted on a tripod in about 17 m initial depth, near the lake's deepest point (black circle, Figure 1). The ADP, mounted at elevation  $z = 1.5$  m above the bed, measured 10-minute-averaged velocity every 0.7 m between  $z = 3$  m and the surface (where  $z = 15.5$ –17 m). Velocities

measured at  $z > 13.5$  m were contaminated by acoustic sidelobe reflections from the surface, and were discarded.

[9] Temperature was measured by continuously raising and lowering an RBR XR-620 CTD from a traveling boat. The CTD sampled at 6 Hz, while the boat traveled at about  $0.3 \text{ ms}^{-1}$ . On 13 September, a temperature transect was collected along the entire length of the lake (green line, Figure 1e), from 0.5 m depth to the bed. Twelve across-lake transects of the hypolimnion (between about 9 m depth and the lakebed) were collected on 8–9 September (red line, Figure 1e). CTD downcasts were interpolated to estimate along-lake and across-lake temperature cross-sections.

### 3. Vertical Propagation

[10] Velocities were predominantly oriented along-lake ( $144^\circ$  clockwise from north, Figure 1e), with magnitude  $0.01$ – $0.02 \text{ ms}^{-1}$  root-mean-square (Figure 2a). Velocity fluctuations were significant at cyclic (as opposed to radian) frequencies  $\sigma$  up to about  $3 \text{ day}^{-1}$ , with near-diurnal periods dominating (Figure 2b).

[11] Velocities band-passed between  $0.7 \text{ day}^{-1}$  and  $1.4 \text{ day}^{-1}$  showed small vertical wavelengths ( $\lambda_z = 4$ –7 m) and zero-crossings at 3–4 vertical locations, as would be expected for vertical modes 3–4 (Figure 2c). However, unlike vertically standing non-dissipative modes, the observed velocities showed upward phase propagation. Vertical phase speeds  $c_z$  were consistent with the linear shallow water WKB prediction [Phillips, 1977] for waves with along-lake wavelength  $\lambda_x = 3000$  m:

$$c_z = 2\pi\sigma^2\lambda_x/\bar{N} \quad (1)$$

(dotted lines, Figure 1e). Here  $\lambda_x$  was chosen to fit observations, the Coriolis acceleration was neglected, and the Brunt-Väisälä frequency  $\bar{N} = [-(g/\bar{\rho})\partial\bar{\rho}/\partial z]^{1/2}$  [Phillips, 1977] was calculated from the along-lake average of measured density  $\bar{\rho}$  (section 4) with  $g = 9.8 \text{ ms}^{-2}$ . The fitted horizontal wavelength  $\lambda_x$  is about twice the lake length at 6 m depth (Figure 1e).

[12] Consistent with observed upward phase propagation, on days 245–247, 249–251 and 253–254 wave groups can be seen propagating downward at the theoretical vertical group velocity

$$c_{g,z} = -c_z, \quad (2)$$

although propagation is unclear for a prolonged group on days 256–259 (solid lines, Figure 2c). Wave groups took about 1.7 days to propagate from near the lake surface to near the bed ( $z = 13$  m to 3 m), and  $c_{g,z}$  was about  $10^{-4} \text{ ms}^{-1}$ . The mean energy flux ( $Ec_{g,z} \approx 2Kc_{g,z}$ , where  $E$  = total energy,  $K$  = kinetic energy) carried toward the bed by propagating waves has magnitude

$$F_z = \rho\langle|u|^2\rangle|c_{g,z}| \sim 2.6 \times 10^{-5} \text{ Wm}^{-2}, \quad (3)$$

where angle brackets denote an average and  $\langle|u|^2\rangle \approx (0.016 \text{ ms}^{-1})^2$  (Figure 2a).

[13] The simple model represented by (1)–(3) is sufficient to show that the observed motions are vertically propagating internal waves and to provide a rough energy flux estimate. However, this model is exact only for linear WKB waves in

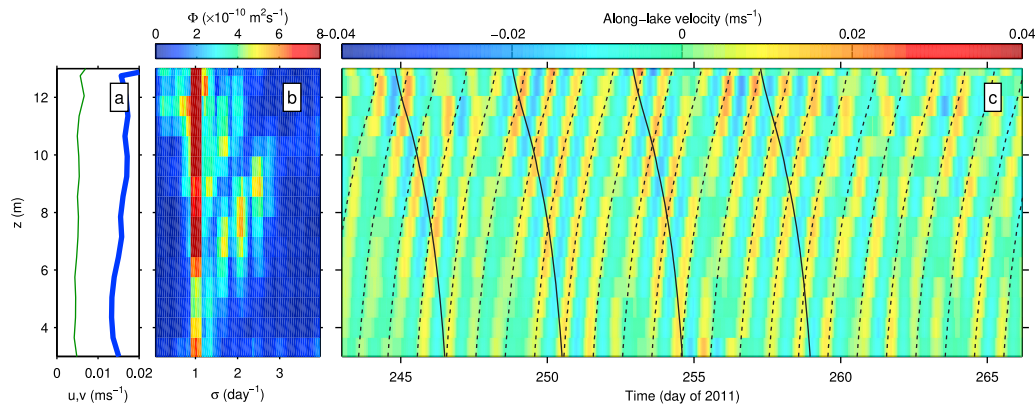


**Figure 2.** Vertical profiles of (a) root-mean-square along-lake velocity  $u$  (thick blue curve) and across-lake velocity  $v$  (thin green curve), (b) power spectral density  $\Phi$  of  $u$ , (c) time series of  $u$  (band-passed between 0.7 and 1.4 cycles/day). In Figure 2c, dotted and solid lines respectively show theoretical vertical propagation of wave phases and wave groups.

a lake with vertical end walls and total absorption of energy at the lakebed. A more complete but more complex simulation could be achieved using a numerical model [Becherer and Umlauf, 2011]. Numerical modeling is not attempted here.

#### 4. Along-Lake Section

[14] On the afternoon of 13 September, 1–5 m from the surface, isotherms sloped down to the southeast (dashed white line 1, Figure 3a), likely a result of southeastward winds (wind speed was not measured, but wind direction was noted by observers). Isotherm slope reversed, tilting up to the southeast, at 5–9 m depth (dashed line 2), and reversed again, tilting down to the southeast, at depths exceeding 9 m (dashed line 3). Near-surface water velocity was oriented downwind, but velocity reversed several times along the vertical profile (black bars, Figure 3a). In contrast to the reversals of isotherm tilt along surface-to-bed vertical profiles, isotherm tilts did not reverse on horizontal lines along the lake. These observations are consistent with the inference (section 3) that dominant motions are waves with small vertical wavelengths and with horizontal wavelengths exceeding the lake length.

[15] Stratification, measured by the local Brunt-Väisälä frequency  $N = [-(g/\rho)\partial\rho/\partial z]^{1/2}$  (where  $\rho$  = density calculated from local temperature, as opposed to the along-lake-averaged density  $\bar{\rho}$  used to calculate  $\bar{N}$ , equation (1)) was intense at the base of the thermocline (1–6 m), particularly over a sill near the southeast end of the lake (Figure 3b). Above the thermocline, stratification was near-zero. Below about 8 m depth, stratification grew weaker with increasing depth. Below the surface mixed layer, most  $N$  values ranged between 0.01 and 0.05  $s^{-1}$ , much greater than  $\sigma \approx 1 \times 10^{-5} s^{-1}$ , justifying the shallow water approximation used in (1).

[16] The energy of small amplitude, shallow water internal waves propagates along rays at angle

$$\theta_c \approx 2\pi\sigma/\bar{N} \quad (4)$$

radians from horizontal. Bed slopes are supercritical if greater than  $\theta_c$ , and subcritical if less than  $\theta_c$ . Most (70%) of

the lakebed was supercritical (pink, green, and blue lines, Figure 3b). Consequently, over most of Lacamas Lake, internal wave energy is reflected downward on reaching the lakebed.

[17] Intensified stratification coincided with an internal wave ray (with slope  $\theta_c$ , black curve in Figure 3b) emanating from a sill near the southeast end of the lake. Such intensification might indicate focusing of downward-propagating waves by reflection from the sill's near-critical bed. However, no corresponding intensification of velocity was observed (Figure 2).

#### 5. Across-Lake Sections

[18] Between 9 and 14 m depth, vertical shear was related to across-lake isotherm slope by the thermal wind balance [Gill, 1982]

$$\partial u/\partial z = (\rho f)^{-1} g \partial \rho/\partial y, \quad (5)$$

where  $y$  = across-lake coordinate and  $f$  = Coriolis parameter (Figures 3c and 3d). The implied approximate cancelation of Coriolis accelerations by across-lake baroclinic pressure gradients justifies the neglect of Coriolis in sections 3 and 4. Such cancelation likely develops as these subinertial motions are constrained to flow predominantly along, rather than across, the narrow lake (Figure 2a). Vertically propagating internal Kelvin waves (of both coastal [Drushka et al., 2010] and equatorial [Wunsch, 1977; Luyten and Roemmich, 1982] varieties) exhibit a similar cancelation of Coriolis accelerations, and are governed by equations analogous to (1)–(3). The across-shore amplitude decay characterizing Kelvin waves is limited here by the narrowness of the lake.

#### 6. Discussion and Conclusions

[19] Like lowest-horizontal-mode seiches, internal waves in Lacamas Lake had horizontal wavelengths exceeding the metalimnion length. However, unlike standing seiches described by previous researchers, the observed waves propagated vertically, carrying energy down toward the lakebed.

[20] The small vertical wavelengths observed were likely determined by the lake's small size and strong stratification.



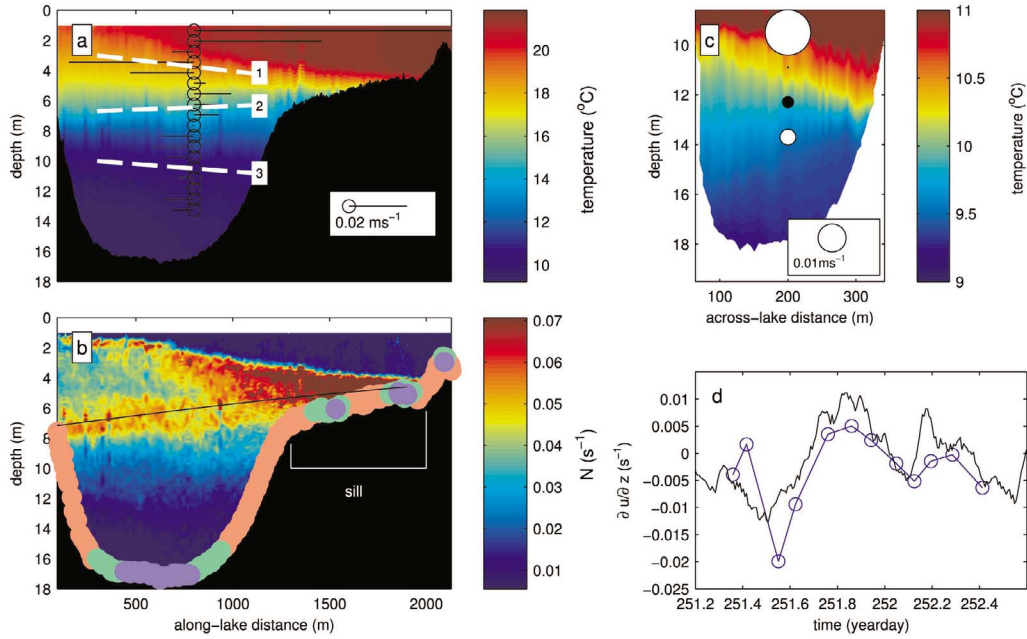


**Figure 3.** Along- and across-lake sections, together with vertical shear predicted from across-lake sections. (a) Velocity (black bars) and along-lake temperature section (color). White dashed lines 1–3 mark isotherm slopes. (b) Buoyancy frequency  $N$ , with super- and sub- and near-critical bed slopes (respectively  $\theta > 2\theta_c$ ,  $\theta < \theta_c/2$ , and  $\theta_c/2 < \theta < 2\theta_c$ ) marked by pink, blue, and green lines. Black curve marks an internal wave ray. (c) Across-lake temperature section (measured at year-day 251.55, color) and along-lake velocity (white and black circles mark flow into and out of page, with circle diameter proportional to velocity). (d) Vertical shear (averaged between 9 and 14 m depth) measured by ADP (black curve) and predicted from successive across-lake temperature gradients using thermal wind relation (5) (blue curve and circles).

Setting  $\lambda_x = 2L$  (where  $L$  = lake length), noting that  $c_z = \sigma \lambda_z$ , and re-arranging (1) yields  $\lambda_z = 4\pi\sigma L/N$ . Therefore, for diurnal forcing with  $\sigma = (24 \text{ hours})^{-1}$ , small vertical wavelengths are favored in short (low  $L$ ), strongly-stratified lakes. Previous observations show a tendency for short vertical wavelengths to be observed in small or medium lakes [LaZerte, 1980; Weigand and Chamberlain, 1987; Münnich et al., 1992; Vidal et al., 2005, 2008; Vidal and Casamitjana, 2007; Pannard et al., 2011; Lorrain et al., 2011].

[21] Development of small vertical scales might have been reinforced by wave focusing, theoretically predicted where waves reflect from near-critical bed slopes. Consistent with this prediction, an along-lake transect revealed slightly intensified stratification along a ray emerging from a near-critical sill (section 4). However, results were inconclusive because only a single along-lake temperature transect was measured, and measured velocities were not intensified along this beam. Sills have previously been found to intensify seiche motion [Fricker and Nepf, 2000] and radiate waves beams associated with localized dissipation [Boehrer and Stevens, 2005].

[22] Theory (4) predicts widespread supercritical slopes and downward reflection when  $D = (NH)/(\pi\sigma L)$  exceeds about one (approximating the bed slope with  $2H/L$ , where  $H$  = lake depth). For Lacamas Lake,  $D \approx 8$  (evaluating  $N$  from the surface-to-bed temperature difference) and most of the lakebed was supercritical (section 4). For large  $D$ , wave rays must repeatedly cross the lake and reflect from endwalls while propagating from surface to bed (or from bed to surface). For Lacamas Lake, ray tracing (not shown, but

following the approach used to draw the ray in Figure 3b) indicates that 3–4 endwall reflections occur during vertical propagation. Therefore, any upward propagating energy present must repeatedly cross the vertical profile of ADP measurements while propagating to the surface. Since downward propagating energy dominated the entire measured ADP-profile, we conclude that most wave energy was not reflected and carried back to the surface, and must instead have been lost in the hypolimnion.

[23] Dissipation, possibly in the bottom boundary layer, might account for the lost energy. For reflection from the subcritical portion of the bed to be weak, boundary layer dissipation must be substantial compared with the downward wave energy flux. Since dissipation is of order  $\rho C_D \langle |u|^3 \rangle$  (we assume a generic value  $C_D \sim 2.5 \times 10^{-3}$  for the bottom drag coefficient [Simpson and Hunter, 1974]), it follows from (3) that strong reflection is expected only if

$$R = \left(\frac{8}{\pi}\right)^{1/2} \frac{C_D \langle |u|^2 \rangle^{1/2}}{|c_{g,z}|} \ll 1, \quad (6)$$

where we applied the simplification  $\langle |u|^3 \rangle = (8/\pi)^{1/2} \langle |u|^2 \rangle^{3/2}$  (exact for Gaussian velocity). For Lacamas lake,  $\langle |u|^2 \rangle^{1/2} \sim 1.6 \times 10^{-2} \text{ ms}^{-1}$  and  $|c_{g,z}| \sim 10^{-4} \text{ ms}^{-1}$  (section 3), so  $R \sim 0.6$ . Consequently, substantial boundary layer absorption is predicted during a single reflection. Furthermore, six to eight endwall reflections occur during vertical propagation (3–4 each during upward and downward propagation), each contributing additional dissipation. For narrow lakes in general,

absorption and propagation are favored by numerous endwall reflections (large  $D$ ), and by small vertical group velocity (6). From (2), the vertical component of group velocity has magnitude  $\sigma\lambda_z$ , so vertical propagation is favored for waves with small vertical wavelengths. For a lowest horizontal mode (with  $\lambda_x \sim 2L$ ), from (1), (2) and (6),  $R \sim (2\pi)^{-3/2} C_D \langle |u|^2 \rangle^{1/2} \bar{N} / (\sigma^2 L)$  and absorption is favored in short lakes with strong near-bed stratification. For lakes that are broad (compared with the internal Rossby Radius), Coriolis accelerations will complicate the analysis.

[24] Regardless of the complex boundary layer processes that might control wave reflection [Lorke et al., 2005; Lorrai et al., 2011], near bed dissipation can not exceed the energy supplied by incident waves. Therefore, in cases with strong vertical propagation, boundary layer dissipation may be limited by the wave energy flux ('wave-limited dissipation'), which can be evaluated simply as wave energy multiplied by group velocity (about  $2.6 \times 10^{-5} \text{ W m}^{-2}$  in this case).

[25] The above discussion suggests that downward reflection, boundary layer absorption, vertical propagation, and wave-limited dissipation are favored by short lake lengths and strong near-bed stratification.

[26] Near-bed wave absorption limits resonance and focusing toward IWAs, because both require repeated cycles of vertical propagation. In the absence of resonance, dominant wave frequencies are expected to reflect dominant forcing frequencies. Therefore, the diurnal wave period might have resulted from diurnal wind forcing (common near this lake [Sharp and Mass, 2004] and measured on this lake by an Onset Hobo weather station during September 2009 (not shown)).

[27] Since wave energy took 1.7 days to reach the lakebed, boundary layer dissipation and mixing in Lacamas Lake are expected to lag wind events by about 1.7 days.

[28] **Acknowledgments.** John Harrison contributed to planing and execution of fieldwork, and provided valuable comments on this paper. Further fieldwork assistance was provided by Abby Lunstrum, Homer Adams, Michelle McCrackin, Rebecca Martin, Andrew Harwood, John Gibbons, Matthew Schullt, and Maria Glavin. We thank the Lacamas Shores Neighborhood Association and the Camas Moose Lodge for lake access. Funding was provided by the National Science Foundation, the US Geological Survey, and the State of Washington.

[29] The Editor thanks Leo Maas and an anonymous reviewer for their assistance in evaluating this paper.

## References

- Becherer, J. K., and L. Umlauf (2011), Boundary mixing in lakes: 1. Modeling the effect of shear-induced convection, *J. Geophys. Res.*, *116*, C10017, doi:10.1029/2011JC007119.
- Boehrer, B., and C. Stevens (2005), Ray waves in a pit lake, *Geophys. Res. Lett.*, *32*, L24608, doi:10.1029/2005GL024678.
- Brink, K. H., and J. Allen (1978), On the effect of bottom friction on barotropic motion over the continental shelf, *J. Phys. Oceanogr.*, *8*, 919–922.
- Cacchione, D., L. Pratson, and A. Ogston (2002), The shaping on continental slopes by internal tides, *Science*, *296*, 724–727.
- Drushka, K., J. Sprintall, and S. Gille (2010), Vertical structure of Kelvin waves in the Indonesian Throughflow exit passages, *J. Phys. Oceanogr.*, *40*, 1965–1987.
- Eriksen, C. C. (1982), Observations of internal wave reflection off sloping bottoms, *J. Geophys. Res.*, *87*, 525–538.
- Fricke, P., and H. Nepf (2000), Bathymetry, stratification, and internal seiche structure, *J. Geophys. Res.*, *105*, 14,237–14,251.
- Gill, A. E. (1982), *Atmosphere-ocean Dynamics*, Academic, London.

- Gómez-Giraldo, A., J. Imberger, and J. P. Antenucci (2006), Spatial structure of the dominant basin-scale internal waves in Lake Kinneret, *Limnol. Oceanogr.*, *51*, 229–246.
- Hazewinkel, J., C. Tsimriti, L. R. Maas, and S. B. Dalziel (2010), Observations on the robustness of internal wave attractors to perturbations, *Phys. Fluids*, *22*, 107102, doi:10.1063/1.3489008.
- LaZerte, B. D. (1980), The dominating higher order vertical modes of the internal seiche in a small lake, *Limnol. Oceanogr.*, *25*, 846–854.
- Lorke, A., F. Peeters, and A. Wüest (2005), Shear-induced convective mixing in bottom boundary layers on slopes, *Limnol. Oceanogr.*, *50*, 1612–1619.
- Lorrai, C., L. Umlauf, J. K. Becherer, A. Lorke, and A. Wüest (2011), Boundary mixing in lakes: 2. Combined effects of shear- and convectively induced turbulence on basin-scale mixing, *J. Geophys. Res.*, *116*, C10018, doi:10.1029/2011JC007121.
- Luyten, J. R., and D. H. Roemmich (1982), Equatorial currents at semi-annual period in the Indian Ocean, *J. Phys. Oceanogr.*, *12*, 406–413.
- Maas, L. R., and F.-P. Lam (1995), Geometric focusing of internal waves, *J. Fluid Mech.*, *300*, 1–41.
- Maas, L. R., D. Benielli, J. Sommeria, and F.-P. A. Lam (1997), Observations of an internal wave attractor in a confined, stably stratified fluid, *Nature*, *388*, 557–561.
- MacIntyre, S., and R. Jellison (2001), Nutrient fluxes from upwelling and enhanced turbulence at the top of the pycnocline in Mono Lake, California, *Hydrobiologia*, *466*, 13–29.
- Mortimer, C. (1952), Water movements in lakes during summer stratification, *Philos. Trans. R. Soc. London, Ser. B*, *236*, 355–398.
- Münnich, M., A. Wüest, and D. Imboden (1992), Observations of the second vertical mode of the internal seiche in an alpine lake, *Limnol. Oceanogr.*, *37*, 1705–1719.
- Pannard, A., B. E. Beisner, D. F. Bird, J. Braun, D. Planas, and M. Bormans (2011), Recurrent internal waves in a small lake: Potential ecological consequences for metalimnetic phytoplankton populations, *Limnol. Oceanogr.*, *1*, 91–109.
- Phillips, O. (1977), *The Dynamics of the Upper Ocean*, 2nd ed., Cambridge Univ. Press, Cambridge, U. K.
- Pierson, D. C., and G. A. Weyhenmeyer (1994), High resolution measurements of sediment resuspension above an accumulation bottom in a stratified lake, *Hydrobiologia*, *284*, 43–57.
- Serra, T., L. J. Vidal, X. Casamitjana, M. Soler, and J. Colomer (2007), The role of surface vertical mixing in phytoplankton distribution in a stratified reservoir, *Limnol. Oceanogr.*, *52*, 620–634.
- Sharp, J., and C. F. Mass (2004), Columbia Gorge gap winds: Their climatological influence and synoptic evolution, *Weather Forecast.*, *19*, 970–992.
- Shimizu, K., and J. Imberger (2009), Damping mechanisms of internal waves in continuously stratified rotating basins, *J. Fluid Mech.*, *637*, 137–172.
- Simpson, J., and J. Hunter (1974), Fronts in the Irish Sea, *Nature*, *250*, 404–406.
- Sorensen, J., M. Sydor, H. Huls, and M. Costello (2004), Analysis of Lake Superior seiche activity for estimating effects on pollution transport in the St. Louis River estuary under extreme conditions, *J. Great Lakes Res.*, *30*, 293–300.
- Thorpe, S. A. (1998), Some dynamical effects of internal waves and the sloping sides of lakes, in *Physical Processes in Lakes and Oceans, Coastal Estuarine Stud.*, vol. 54, edited by J. Imberger, pp. 441–460, AGU, Washington, D. C.
- Vidal, J., and X. Casamitjana (2007), The seasonal evolution of high vertical mode internal waves in a deep reservoir, *Limnol. Oceanogr.*, *56*, 2656–2667.
- Vidal, J., X. Casamitjana, J. Colomer, and T. Serra (2005), The internal wave field in Sau reservoir: Observation and modeling of a third vertical mode, *Limnol. Oceanogr.*, *50*, 1326–1333.
- Vidal, J., F. J. Rueda, and X. Casamitjana (2008), Forced resonant oscillations as a response to periodic winds in a stratified reservoir, *J. Hydraul. Eng.*, *134*, 416–425.
- Weigand, R. C., and V. Chamberlain (1987), Internal waves of the second vertical mode in a stratified lake, *Limnol. Oceanogr.*, *32*, 29–42.
- Wüest, A., and A. Lorke (2003), Small-scale hydrodynamics in lakes, *Annu. Rev. Fluid Mech.*, *35*, 373–412.
- Wunsch, C. (1977), Response of an equatorial ocean to periodic motion, *J. Phys. Oceanogr.*, *7*, 497–511.

B. Deemer and S. M. Henderson, School of the Environment, Washington State University Vancouver, 14204 NE Salmon Creek Ave., Vancouver, WA 98686, USA. (steve\_henderson@vancouver.wsu.edu)